

弦-梁耦合系统的动力学行为分析

王霞^{1,2}, 李建平²

(1. 郑州大学 数学系, 郑州 450001; 2. 河南工程学院 数理科学系, 郑州 451191)

摘要: 研究了弦-梁耦合系统在初始平衡解处的稳定性与分岔情况, 给出了特征值随阻尼参数的变化情况, 并利用稳定性分析和特征值分析等解析方法, 得到了初始平衡解、周期解和拟周期解的稳定边界以及导致 Hopf 分岔和 2 维胎面等分岔解的临界分岔曲线。最后, 利用数值模拟方法研究了弦-梁耦合系统的稳定性与分岔情况。

关键词: 弦-梁耦合系统; 稳定性; 分岔; 周期解

中图分类号: TU318; O322

文献标识码: A

DOI: 10.13465/j.cnki.jvs.2014.05.010

Dynamical analysis of a string-beam coupled system

WANG Xia^{1,2}, LI Jian-ping²

(1. Department of Mathematics, Zhengzhou University, Zhengzhou 450001, China;

2. Department of Mathematical and Physical Sciences, Henan Institute of Engineering, Zhengzhou 451191, China)

Abstract: The stability and bifurcations of a string-beam coupled system at its initial equilibrium solution were investigated in detail with a combination of analytical and numerical methods. The variation of the eigenvalues versus parameters was investigated. Based on the averaged equation, the expressions for the critical bifurcation lines leading to incipient and secondary bifurcations, such as, Hopf bifurcation and 2-D tori, were obtained. Numerical simulations of these bifurcation cases were also carried out, whose results agreed well with the analytical ones, at least qualitatively.

Key words: a string-beam coupled system; stability; bifurcation; periodic solution

近几十年来,弦-梁耦合系统由于其其在机械工程、建筑、航空航天以及汽车等领域都有广泛的应用,引起了国内外学者的广泛关注,已经有了大量的文献和研究成果,比如 Cheng 等^[1]研究了通讯工程中的光纤耦合器, Wang 等^[2]用有限元方法研究了桥梁工程中的斜拉索桥, Fung 等^[3-5]分别用数值和理论分析的方法研究了索-梁组合结构的非线性行为, 丁虎等^[6]研究了轴向变速黏弹性梁的横向振动稳定性, Chen 等^[7]研究了高维轴向变速黏弹性梁的分岔和混沌运动, Ghayesh 等^[8]讨论了横向简谐激励力下的轴向运动梁的临界动力学行为, Cao 等^[9-10]分别用数值分析和全局摄动等方法讨论了弦-梁耦合系统的混沌动力学, 文献[11]利用多尺度法研究了 3:1 内共振条件下的弦-梁耦合系统的非线性动力学行为。

本文主要研究二自由度弦-梁耦合系统的稳定性和分岔行为。首先讨论了系统在平凡解处的稳定性,

并给出了特征值随阻尼参数的变化情况。其次, 利用理论分析方法研究了初始平衡解、周期解和拟周期解的稳定性以及导致 Hopf 分岔和 2 维胎面等分岔解的临界分岔曲线。

1 问题描述

考虑弦-梁耦合系统的非线性横向振动, 如图 1, 文献[10]利用单模态 Galerkin 方法, 得到弦-梁耦合系统的无量纲运动的非线性常微分控制方程为:

$$\begin{aligned} \ddot{y}_1 + \mu_1 \dot{y}_1 + (\beta_1 K^{*4} - \beta_2 l_2) y_1 - \beta_4 g_{22} l_{11} y_2^2 y_1 + \\ F_2 l_{11} \cos(\Omega_2 t) \cdot y_1 - (\beta_3 g_{11} l_{11} + \beta_4 g_{11} l_{11}) y_1^3 - \\ 2\beta_4 g_{22} l_{11} y_2 y_1^2 = f_{11} \cos \Omega_1 t \end{aligned} \quad (1a)$$

$$\begin{aligned} \ddot{y}_2 + \lambda_{21} \ddot{y}_1 + \mu_2 \dot{y}_2 + \mu_2 \lambda_{21} \dot{y}_1 - \alpha_1 l_{22} y_2 - \\ \alpha_1 l_{12} y_1 - \alpha_2 g_{22} l_{22} y_2^3 - \alpha_2 (g_{22} l_{22} + \\ 2g_{21} l_{22}) y_2^2 y_1 - \alpha_2 (g_{11} l_{22} + 2g_{21} l_{12}) y_2 y_1^2 - \\ \alpha_2 g_{11} l_{12} y_1^3 = f_{12} \cos \Omega_1 t \end{aligned} \quad (1b)$$

其中参数意义详见文献[10]。为了便于下面讨论, 引入记号 $X = \{y_1, y_2, \dot{y}_1, \dot{y}_2\}^T$, 则方程(1)可写为如下矩阵形式:

$$\dot{X} = A(\mu_1, \lambda_{21}, \dots)X + F(\mu_1, \lambda_{21}, \dots, X) \quad (2)$$

其中:

基金项目: 国家自然科学基金资助项目(11172125); 河南省自然科学基金研究项目(132300410309); 河南省教育厅自然科学研究项目(2011B110006); 河南工程学院博士基金项目(D2010008)

收稿日期: 2011-10-17 修改稿收到日期: 2012-08-09

第一作者 王霞女, 博士, 副教授, 1981年1月生

$$A = \begin{bmatrix} 0 & I \\ -M^{-1}K' & -M^{-1}C \end{bmatrix}$$

$$F(\mu_1, \lambda_{21}, \dots, X) = \begin{bmatrix} f_1(y_1, y_2, \dot{y}_1, \dot{y}_2) \\ f_2(y_1, y_2, \dot{y}_1, \dot{y}_2) \end{bmatrix}$$

$$M = \begin{bmatrix} 1 & 0 \\ \lambda_{21} & 1 \end{bmatrix}, \quad C = \begin{bmatrix} \mu_1 & 0 \\ \mu_2 \lambda_{21} & \mu_2 \end{bmatrix}$$

$$K' = \begin{bmatrix} (\beta_1 K^{*4} - \beta_2 l_2) + F_2 l_{11} \cos(\Omega_2 t) & 0 \\ -\alpha_1 l_{12} & -\alpha_1 l_{22} \end{bmatrix} =$$

$$\begin{bmatrix} \alpha_2 & 0 \\ -\alpha_1 l_{12} & -\alpha_1 l_{22} \end{bmatrix}$$

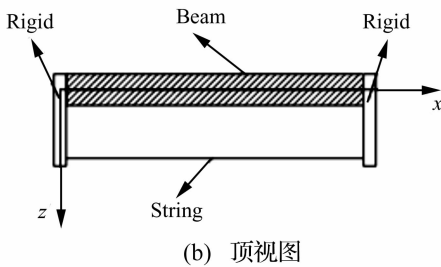
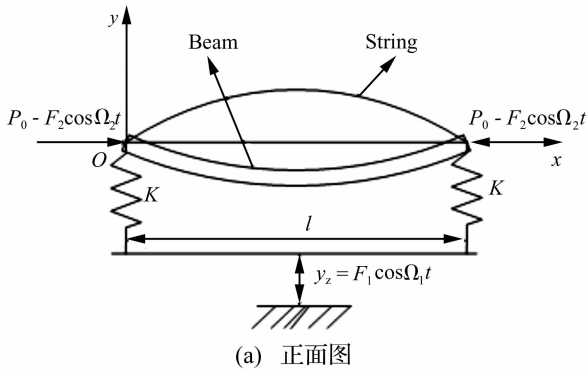


图1 模型示意图

Fig. 1 Schematics of the model

2 稳定性分析

考虑系统外激励项和参数激励项的振幅均为零的情况,即 $F_2 = 0, f_{11} = f_{12} = 0$, 此时系统(2)在平凡解 $\{y_1, y_2, \dot{y}_1, \dot{y}_2\}^T = (0, 0, 0, 0)$ 处的 Jacobi 矩阵的特征方程为:

$$P(\lambda) = a_0 \lambda^4 + a_1 \lambda^3 + a_2 \lambda^2 + a_3 \lambda + a_4 = 0 \quad (3)$$

其中 $a_0 = 1, a_1 = \mu_1 + \mu_2,$

$a_2 = \alpha_2 - \alpha_1 l_2 + \mu_1 \mu_2, a_3 = \alpha_2 \mu_2 - \alpha_1 l_2 \mu_1,$

$a_4 = -\alpha_2 \alpha_1 l_2$ 。由 Routh-Hurwitz 判据,零解的稳定条件为:

$$a_1 > 0, a_4 > 0$$

$$e_2 = a_1 a_2 - a_0 a_3 =$$

$$\mu_1 \mu_2^2 + \mu_1 \alpha_2 + \mu_1^2 \mu_2 - \mu_2 \alpha_1 l_2 > 0$$

$$e_3 = e_2 a_3 - a_1^2 a_4 =$$

$$(\alpha_2 - \alpha_1 l_2) \mu_1^2 \mu_2^2 + (\alpha_1^2 l_2^2 + \alpha_2^2 +$$

$$2\alpha_1 \alpha_2 l_2) \mu_1 \mu_2 + \mu_1 \mu_2^3 \alpha_2 - \mu_1^3 \mu_2 \alpha_1 l_2 > 0$$

由上述稳定性条件,可得系统的稳定性图,如图(2),其中考虑 $\alpha_2 = 0.2, \mu_2 = 0.1, l_2 = 0.7$ 。

根据文献[12,13],令:

$$K = a_0^2 \left(a_0 a_4 - \frac{1}{4} a_1 a_3 + \frac{1}{12} a_2^2 \right) -$$

$$12 \left(\frac{1}{6} a_0 a_2 - \frac{1}{16} a_1^2 \right)^2 = 0 \quad (4)$$

由图(2)可知,系统在平凡解附近的局部性质有如下几种情况:

(1) 纯发散: $a_4 > 0, a_2 < 0, K < 0$ 。此时特征方程(3)有四个实特征值,其中两个特征值是正的,另两个特征值是负的。(图2中阴影部分。)

(2) 颤振: $K > 0$ 或者 $a_2 > 0, a_4 > 0, K < 0, e_3 < 0$ 。此时特征方程(3)有两对复共轭特征值,其中一对复共轭特征值具有正实部,另一对复共轭特征值具有负实部。(图2中水平线部分。)

(3) 衰减振荡型发散: $a_4 < 0$ 和 $e_3 > 0$ 或者 $e_3 < 0$ 和 $a_3 < 0$ 。此时特征方程(3)有一对具有负实部的复共轭特征值和两个相反符号的实特征值。(图2中斜线部分。)

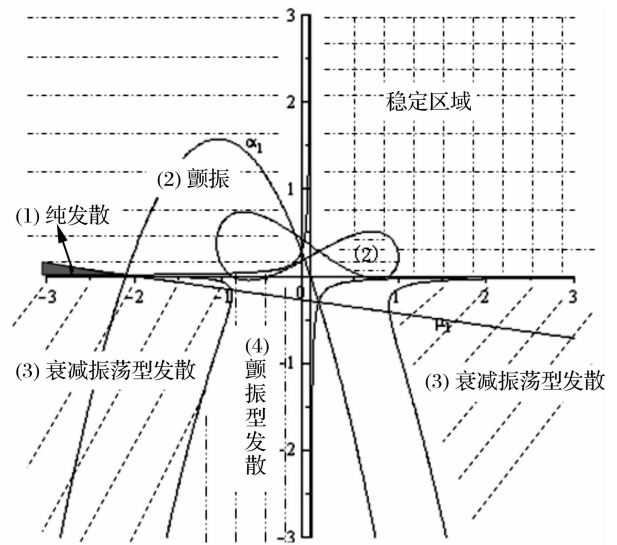


图2 零解的稳定图

Fig. 2 Stability of the zero-solution

(4) 颤振型发散: $a_4 < 0, e_3 < 0, a_3 > 0$ 。此时特征方程(3)有一对具有正实部的复共轭特征值和两个相反符号的实特征值。(图2中竖线部分。)

(5) 其他情况: 一对纯虚根和一对具有负实部的复共轭特征值,此时要求 $e_3 = 0, a_3 > 0$ 和 $e_2 > 0$; 当 $e_3 = 0, a_4 = 0$ 时,特征方程(3)有一对纯虚根和两个零根等等。

接下来,当参数 $\alpha_1 = 10, l_2 = -0.7, \alpha_2 = 0.2$, 参考文献[14]中的方法,讨论特征值随阻尼参数的变化情

况。此时,特征值可表示为:

$$\lambda_{1,2} = -0.5\mu_1 \pm 0.1 \sqrt{25\mu_1^2 - 20} \quad (5a)$$

$$\lambda_{3,4} = -0.5\mu_2 \pm 0.5 \sqrt{25\mu_2^2 - 28} \quad (5b)$$

由上式可知,当 $\mu_1 < 0$ 或 $\mu_2 < 0$,零解是不稳定的。当 $\mu_1 = 0$ 或 $\mu_2 = 0$,特征值出现一对纯虚根,即出现 Hopf 分岔。特征值变化情况如图 3 和图 4。对于 $\lambda_{1,2}$,由图 3 知,随着 μ_1 的增加, $\lambda_{1,2}$ 在 $\mu_1 = -2\sqrt{5}/5$ 处由两个正的实特征值变为一个正的实特征值,随之变为一对具有正实部的复共轭特征值,在 $\mu_1 = 0$ 时发生 Hopf 分岔,然后,出现两个具有负实部的复共轭特征值,当 $\mu_1 = 2\sqrt{5}/5$ 时,特征值由一对复特征值变为两个负实特征值。同理,对于 $\lambda_{3,4}$,由图 4 知,随着 μ_2 的增加, $\lambda_{3,4}$ 在 $\mu_2 = -2\sqrt{7}$ 处由两个正的实特征值变为一个正的实特征值,随之变为一对具有正实部的复共轭特征值,在 $\mu_2 = 0$ 时发生 Hopf 分岔,然后,出现两个具有负实部的复共轭特征值,当 $\mu_2 = 2\sqrt{7}$ 时,特征值由一对复特征值变为两个负实特征值。

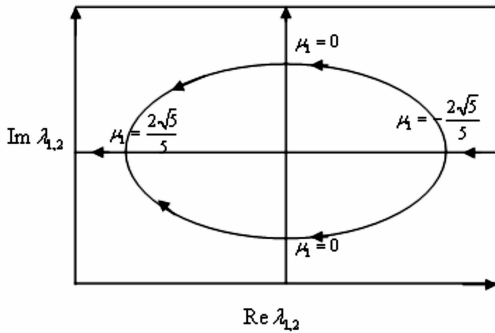


图 3 $\lambda_{1,2}$ 随参数变化示意图

Fig. 3 Schematics of the eigenvalues $\lambda_{1,2}$ of linearized system with the parameters

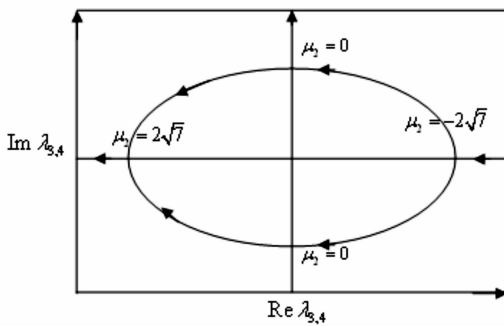


图 4 $\lambda_{3,4}$ 随参数变化示意图

Fig. 4 Schematics of the eigenvalues $\lambda_{3,4}$ of linearized system with the parameters

3 分岔分析

在本节中,利用文献[15-16]的方法,讨论弦-梁耦合系统的稳定性与分岔情况,主要考虑梁和弦之间

的 1:2 内共振,共振关系可表示为:

$$\begin{aligned} \omega_1 &= 2\omega_2, \quad \omega_1^2 = \frac{1}{4}\Omega_2^2 + \varepsilon\sigma_1 \\ \omega_2^2 &= \frac{1}{16}\Omega_2^2 + \varepsilon\sigma_2, \quad \Omega_1 = \frac{1}{4}\Omega_2 \end{aligned} \quad (6)$$

其中 σ_1 和 σ_2 是两个调谐参数。为便于下面分析,令外激励振幅 $f_{11} = f_{12} = 0$ 和 $\Omega_2 = 1$ 。

由参考文献[10]可知系统的平均方程如下:

$$\dot{x}_1 = -\frac{1}{2}\mu_1 x_1 - \sigma_1 x_2 + \frac{1}{2}f_2 x_2 + 2a_{11}(x_3^2 + x_4^2)x_2 + 3a_{14}(x_1^2 + x_2^2)x_2 \quad (7a)$$

$$\dot{x}_2 = -\frac{1}{2}\mu_1 x_2 - \sigma_1 x_1 + \frac{1}{2}f_2 x_1 - 2a_{11}(x_3^2 + x_4^2)x_1 - 3a_{14}(x_1^2 + x_2^2)x_1 \quad (7b)$$

$$\dot{x}_3 = -\frac{1}{2}\mu_2 x_3 - 2\sigma_2 x_4 + 6a_{21}(x_3^2 + x_4^2)x_4 + 4a_{23}(x_1^2 + x_2^2)x_4 \quad (7c)$$

$$\dot{x}_4 = -\frac{1}{2}\mu_2 x_4 + 2\sigma_2 x_3 - 6a_{21}(x_3^2 + x_4^2)x_3 + 4a_{23}(x_1^2 + x_2^2)x_3 - f_{12} \quad (7d)$$

利用如下极坐标变换:

$$\begin{aligned} x_1 &= \rho_1 \cos\theta_1, \quad x_2 = \rho_1 \sin\theta_1 \\ x_3 &= \rho_2 \cos\theta_2, \quad x_4 = \rho_2 \sin\theta_2 \end{aligned} \quad (8)$$

将(7)式转化为极坐标形式:

$$\frac{d\rho_1}{dt} = -\frac{1}{2}\rho_1\mu_1 + \frac{1}{2}\rho_1 f_2 \sin 2\theta_1 \quad (9a)$$

$$\frac{d\rho_2}{dt} = -\frac{1}{2}\rho_2\mu_2 - f_{12} \cos\theta_2 \quad (9b)$$

$$\frac{d\theta_1}{dt} = 3\rho_1^2 a_{14} + \frac{1}{2}f_2 \cos 2\theta_1 + 2a_{11}\rho_2^2 - \sigma_1 \quad (9c)$$

$$\frac{d\theta_2}{dt} = \frac{1}{\rho_2}(4a_{23}\rho_1^2\rho_2 + f_{12}\sin\theta_2 + 6a_{21}\rho_2^3 - 2\sigma_2\rho_2) \quad (9d)$$

3.1 初始平衡解

由系统(7)可知, $(x_1, x_2, x_3, x_4) = (0, 0, 0, 0)$ 是系统的初始平衡解。接下来讨论初始平衡解的稳定性。

系统(7)在初始平衡解处的 Jacobi 矩阵的特征多项式可表示为:

$$\begin{aligned} P(\lambda) &= \left(\lambda^2 + \mu_1\lambda + \frac{1}{4}\mu_1^2 - \frac{1}{4}f_2^2 + \sigma_1^2 \right) \cdot \\ &\quad \left(\lambda^2 + \mu_2\lambda + \frac{1}{4}\mu_2^2 + 4\sigma_2^2 \right) \end{aligned} \quad (10)$$

则初始平衡解的稳定条件为:

$$\frac{1}{4}\mu_1^2 - \frac{1}{4}f_2^2 + \sigma_1^2 > 0, \quad \mu_1 > 0, \quad \mu_2 > 0 \quad (11)$$

令 $L_1: \frac{1}{4}\mu_1^2 - \frac{1}{4}f_2^2 + \sigma_1^2 = 0$, 由方程(10)可知,当

阻尼为正阻尼,而其它参数在曲线 L_1 上时,特征方程有三个负特征值和一个零根,则初始平衡解通过静态分岔失去稳定性。此时初始平衡解将变成一个分岔解,

即单模态解——周期解:

$$\rho_1^2 = \frac{2a_{14}^2\sigma_1^2 + \sqrt{\Delta}}{6a_{14}^2} \quad (12)$$

其中: $\Delta = 4a_{14}^2\sigma_1^2 - a_{14}^2(4\sigma_1^2 + \mu_1^2 - f_2^2)$ 。

3.2 单模态解—周期解 ($\rho_1 \neq 0, \rho_2 = 0$)

在本小节,我们将给出周期解的稳定性条件。首先考虑系统(7)在周期解处的特征多项式如下:

$$P(\lambda) = \left[\lambda^2 + \mu_1\lambda + \frac{1}{4}\mu_1^2 - \frac{1}{4}f_2^2 + 9a_{14}^2\rho_1^4 - 6a_{14}\sigma_1\rho_1^2 + \sigma_1^2 \right] \cdot \left[\lambda^2 + \left[\mu_2\lambda + \frac{1}{4}\mu_1^2 + (2\sigma_2 - 4a_{23}\rho_1^2) \right]^2 \right] \quad (13)$$

由方程(13)可以看出,系统(7)在周期解处的 Jacobi 矩阵的前两个特征值 $\lambda_{1,2}$ 满足方程:

$$\lambda^2 + \mu_1\lambda + \frac{1}{4}\mu_1^2 - \frac{1}{4}f_2^2 + 9a_{14}^2\rho_1^4 - 6a_{14}\sigma_1\rho_1^2 + \sigma_1^2 = 0 \quad (14)$$

则使周期解稳定的条件为 $\frac{1}{4}\mu_1^2 - \frac{1}{4}f_2^2 + 9a_{14}^2\rho_1^4 - 6a_{14}\sigma_1\rho_1^2 + \sigma_1^2 > 0$ 和 $\mu_1 > 0$, 此时这两个特征值为负值。而另两个特征值 $\lambda_{3,4}$ 满足方程

$$\lambda^2 + \mu_2\lambda + \frac{1}{4}\mu_1^2 + (2\sigma_2 - 4a_{23}\rho_1^2)^2 = 0 \quad (15)$$

考虑阻尼为正阻尼时,方程(15)有两个负特征值。当 $\mu_2 = 0$ 且 $1/4\mu_1^2 + (2\sigma_2 - 4a_{23}\rho_1^2)^2 \neq 0$ 时,方程(15)有一对纯虚特征值,即 $\mu_2 = 0$ 为一条临界线。在此临界线上特征值为

$$\lambda_{3,4} = \pm I \sqrt{\frac{1}{4}\mu_1^2 + (2\sigma_2 - 4a_{23}\rho_1^2)^2}$$

因此,周期解失去稳定性,并在直线 $\mu_2 = 0$ 上发生 Hopf 分岔,产生混合模态解,即拟周期解(2 维胎面)。

3.3 混合模态解—拟周期解 ($\rho_1 \neq 0, \rho_2 \neq 0$)

由方程(9)可知系统的拟周期解 ($\rho_1 \neq 0, \rho_2 \neq 0$) 满足如下方程:

$$\mu_1^2 + (2a_{11}\rho_2^2 + 3a_{14}\rho_1^2 - \sigma_1)^2 - f_2^2 = 0 \quad (16a)$$

$$\frac{1}{4}\mu_2^2\rho_2^2 + (4a_{23}\rho_2\rho_1^2 + 6a_{21}\rho_2^3 - 2\sigma_2\rho_2)^2 = 0 \quad (16b)$$

考虑系统(7)在拟周期解处的 Jacobi 矩阵为:

$$J = \begin{bmatrix} b_{11} & b_{12} & b_{13} & b_{14} \\ b_{21} & b_{22} & b_{23} & b_{24} \\ b_{31} & b_{32} & b_{33} & b_{34} \\ b_{41} & b_{42} & b_{43} & b_{44} \end{bmatrix} \quad (17)$$

其中 $b_{11} = -\frac{1}{2}\mu_1 + 3a_{14}\rho_1^2\sin 2\theta_1$

$$b_{12} = \frac{1}{2}f_2 + 6a_{14}\rho_1^2 + 2a_{11}\rho_2^2 - \sigma_1 - 3a_{14}\rho_1^2\cos 2\theta_1$$

$$b_{13} = 4a_{11}\rho_1\rho_2\sin\theta_1\cos\theta_2$$

$$b_{14} = 4a_{11}\rho_1\rho_2\sin\theta_1\sin\theta_2$$

$$b_{21} = \frac{1}{2}f_2 - 6a_{14}\rho_1^2 - 2a_{11}\rho_2^2 + \sigma_1 - 3a_{14}\rho_1^2\cos 2\theta_1$$

$$b_{22} = -\frac{1}{2}\mu_1 - 3a_{14}\rho_1^2\sin 2\theta_1$$

$$b_{23} = -4a_{11}\rho_1\rho_2\cos\theta_1\cos\theta_2$$

$$b_{24} = -4a_{11}\rho_1\rho_2\cos\theta_1\sin\theta_2$$

$$b_{31} = 8a_{23}\rho_1\rho_2\cos\theta_1\sin\theta_2$$

$$b_{32} = 8a_{23}\rho_1\rho_2\sin\theta_1\sin\theta_2$$

$$b_{33} = -\frac{1}{2}\mu_2 + 6a_{21}\rho_2^2\sin 2\theta_2$$

$$b_{34} = -2\sigma_2 + 4a_{23}\rho_1^2 + 12a_{21}\rho_2^2$$

$$-6a_{21}\rho_2^2\cos 2\theta_2 - \frac{b \pm \sqrt{b^2 - 4ac}}{2a}$$

$$b_{41} = -8a_{23}\rho_1\rho_2\cos\theta_1\cos\theta_2$$

$$b_{42} = -8a_{23}\rho_1\rho_2\sin\theta_1\cos\theta_2$$

$$b_{43} = 2\sigma_2 - 4a_{23}\rho_1^2 - 12a_{21}\rho_2^2 + 6a_{21}\rho_2^2\cos 2\theta_2$$

$$b_{44} = -\frac{1}{2}\mu_2 - 6a_{21}\rho_2^2\sin 2\theta_2$$

从而得到系统(7)在拟周期解处的特征多项式为:

$$P(\lambda) = b_0\lambda^4 + b_1\lambda^3 + b_2\lambda^2 + b_3\lambda + b_4 = 0 \quad (18)$$

由 Routh-Hurwitz 判据,拟周期解的稳定条件为:

$$b_1 > 0, b_1b_2 - b_0b_3 > 0, b_4 > 0,$$

$$b_3(b_1b_2 - b_0b_3) - b_1^2b_4 > 0 \quad (19)$$

则可得两条临界分岔曲线,其中一条为:

$$L_2: b_4 = 0 (b_1 > 0, b_1b_2 - b_0b_3 > 0,$$

$$b_3(b_1b_2 - b_0b_3) - b_1^2b_4 > 0) \quad (20)$$

在此临界线上发生静态分岔;另一条临界分岔线为:

$$L_3: b_3(b_1b_2 - b_0b_3) - b_1^2b_4 = 0,$$

$$(b_1 > 0, b_1b_2 - b_0b_3 > 0, b_4 > 0) \quad (21)$$

沿此临界线出现第二次广义 Hopf 分岔,并产生一个 3 维胎面。

4 数值模拟

本节利用 Maple 软件,采用四阶 Runge-Kutta 算法对常微分方程组(7)进行数值模拟。取系统参数 $a_{11} = 45, a_{14} = 24, a_{21} = 25, a_{23} = 16, f_2 = 0.2$, 阻尼参数 $\mu_1 = \mu_2 = 0.2$, 调谐参数 $\sigma_1 = 0.02, \sigma_2 = 0.01$ 时,容易验证,这些参数均满足初始平衡解的稳定条件,则当系统初始值取为 $(x_1, x_2, x_3, x_4) = (0.01, -0.2, 0.1, 0.5)$ 时,可得系统(7)的初始平衡解在 $x_1 - x_2$ 平面内的投影,如图 5。当系统参数变为 $a_{11} = 4.5, a_{14} = 2, a_{21} = 5, a_{23} = 2, f_2 = 2$, 阻尼参数变为 $\mu_1 = \mu_2 = 0.02$, 调谐参数变为 $\sigma_1 = 0.2, \sigma_2 = 0.01$ 时,容易验证,这些参数均满足 Hopf 分岔解的稳定条件,当系统初始值不变,可得系统(7)的 Hopf 分岔解在 $x_1 - x_2$ 平面内的投影,如图 6。

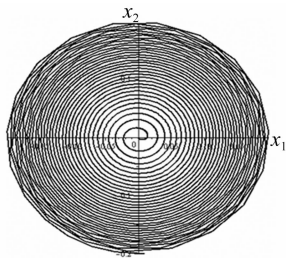


图5 稳定零解的轨道投影
Fig. 5 Trajectory projection
of stability zero-solution

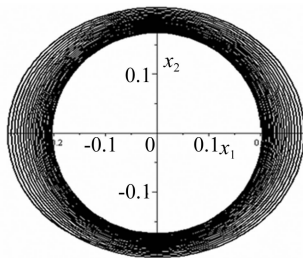


图6 Hopf分岔解的轨道投影
Fig. 6 Trajectory projection
of Hopf solution

5 结 论

研究了一类弦-梁耦合系统在弦与梁之间为2:1内共振条件下的稳定性与分岔行为。给出了几种类型的不稳定点,即纯发散、颤振、衰减振荡型发散、颤振型发散等,并给出了特征值随阻尼参数变化的情况。利用稳定性分析等解析方法,对平均方程进行研究,给出了临界分岔曲线的表达式。研究了系统的静态分叉、Hopf分岔、2维胎面等分岔解及其稳定性。采用Runge-Kutta算法对系统进行数值模拟,验证了我们理论分析的正确性。

参 考 文 献

- [1] Cheng G, Zu J W. Dynamic analysis of an optical fiber coupler in telecommunications [J]. Journal of Sound and Vibration, 2003, 268: 15 - 31.
- [2] Wang P H, Yang C G. Parametric studies on cable-stayed bridges [J]. Computers & Structures, 1996, 60 (2): 243 - 260.
- [3] Fung R F, Lu L Y, Huang S C. Dynamic modeling and vibration analysis of a flexible cable-stayed beam structure [J]. Journal of Sound and Vibration, 2002, 254: 717 - 726.
- [4] Gattulli V, Lepidi M. Nonlinear interactions in the planar dynamics of cable-stayed beam [J]. International Journal of Solids and Structures, 2003, 40: 4729 - 4748.
- [5] Gattulli V, Lepidi M, Macdonald J H G, et al. One-to-two global locale interaction in a cable stayed beam observed through analytical, finite element and experimental models [J]. International Journal of Non-Linear Mechanics, 2005, 40: 571 - 588.

- [6] 丁 虎,陈立群,戈新生. 混杂边界条件下轴向变速运动黏弹性梁参数振动的稳定性[J]. 振动与冲击, 2008, 27 (11): 62 - 63.
- DING Hu, CHEN Li-qun. GE Xin-sheng. Stability in parametric resonance of an axially accelerating viscoelastic beam with hybrid boundary condition [J]. Journal of Vibration and Shock, 2008, 27(11): 62 - 63.
- [7] Chen L H, Zhang W, Yang F H. Nonlinear dynamics of higher-dimensional system for an axially accelerating viscoelastic beam with in-plane and out-of-plane vibrations [J]. Journal of Sound and Vibration, 2010, 329: 5321 - 5345.
- [8] Ghayesh M H, Kafiabad H A, Reid T. Sub-and super-critical nonlinear dynamics of a harmonically excited axially moving beam [J]. International Journal of Solids and Structures, 2012, 49: 227 - 243.
- [9] Cao D X, Zhang W. Analysis on nonlinear dynamics of a string-beam coupled system [J]. International Journal of Nonlinear Sciences and Numerical Simulation, 2005, 6: 47 - 54.
- [10] Cao D X, Zhang W. Global bifurcations and chaotic dynamics for a string-beam coupled system [J]. Chaos, Solitons and Fractals, 2008, 37: 858 - 875.
- [11] Hegazy U H. 3:1 Internal resonance of a string-beam coupled system with cubic nonlinearities [J]. Communications in Nonlinear Science and Numerical Simulation, 2010, 15: 4219 - 4229.
- [12] Herrmann G, Jong I C. On nonconservative stability problems of elastic systems with slight damping [J]. Journal of Applied Mechanics, 1966, March: 125 - 133.
- [13] Thomsen J J. Chaotic dynamics of the partially follower-loaded elastic double pendulum [J]. Journal of Sound and Vibration, 1995, 188(3): 385 - 405.
- [14] Paidoussis M P, Semler C. Nonlinear dynamics of a fluid-conveying cantilevered pipe with an intermediate spring support [J]. Journal of Fluids and Structures, 1993, 7: 269 - 298.
- [15] Bi Q S. Dynamical analysis of two coupled parametrically excited van der Pol oscillators [J]. International Journal of Non-Linear Mechanics, 2004, 39: 33 - 54.
- [16] Bi Q S. Dynamics and modulated chaos for two coupled oscillators [J]. International Journal of Bifurcation and Chaos, 2004, 14(1): 337 - 346.